*设计指南：**TIDA-010075***

*具有 **1.0A** 电流和 **±1.5%** 电压精度的成本优化型电池充电器参考设计*

说明

此参考设计展示了适用于中端或低端扫地机器人的成本优化型板载电池充电器解决方案，具有 1.0A 充电电流和 4.8cm² 布局面积，充电电压精度和充电电流精度分别为 ±1.5%、±3%。本设计具有稳定、平滑的 CC-CV 充电曲线，并使用 4S2P 锂离子电池组完成评估。

资源

TIDA-010075	设计文件夹
TPS54202	产品文件夹
TLV9001	产品文件夹
TVS3300	产品文件夹

Search Our E2E™ support forums

特性

- 适配器输入电压范围为 18.7V 至 28V
- 恒定充电电流：1.0A
- 集成高侧和低侧 FET 的同步降压拓扑
- ±1.5% 充电电压精度
- ±3% 充电电流精度
- 占用布局面积小：4.8cm²
- 工作环境温度：0°C 至 40°C

应用

- 扫地机器人
- 无线真空吸尘器
- 类人机器人

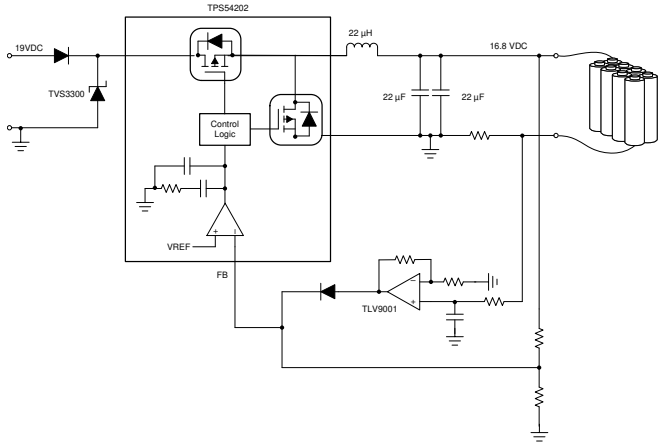

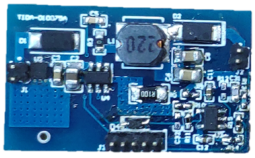

该 TI 参考设计末尾的重要声明表述了授权使用、知识产权问题和其他重要的免责声明和信息。

1 System Description

A vacuum robot, also called a robotic vacuum cleaner, which has been around for about 23 years, is getting more intelligent and automatic. There is an expectation that robots should be able to do a full cleaning cycle before needing to charge again. With more features added in a vacuum robot, such as mopping, audio interaction, navigating thick carpet, and climbing higher thresholds, the power requirement for a full cleaning cycle is increasing, so the battery capacity is becoming bigger, typically from 2600 mAh to 5200 mAh.

Meanwhile, this also increase the requirements for the battery charger. The following items list the general requirements for an onboard charger, which means the charger circuit is implemented on the main board of the robot, which is widely used for almost all brands of vacuum robots around the world:

- High charging current
- Cost effective
- Small size
- High charging voltage accuracy
- High charging current accuracy
- Easy to design

Two different solutions are implemented to achieve an onboard charger. One is an asynchronous buck topology charger which uses the system micro controller (MCU) as the digital controller. 图 1 shows the block diagram of this solution.

图 1. Asynchronous Buck Topology Charger Controlled by System MCU

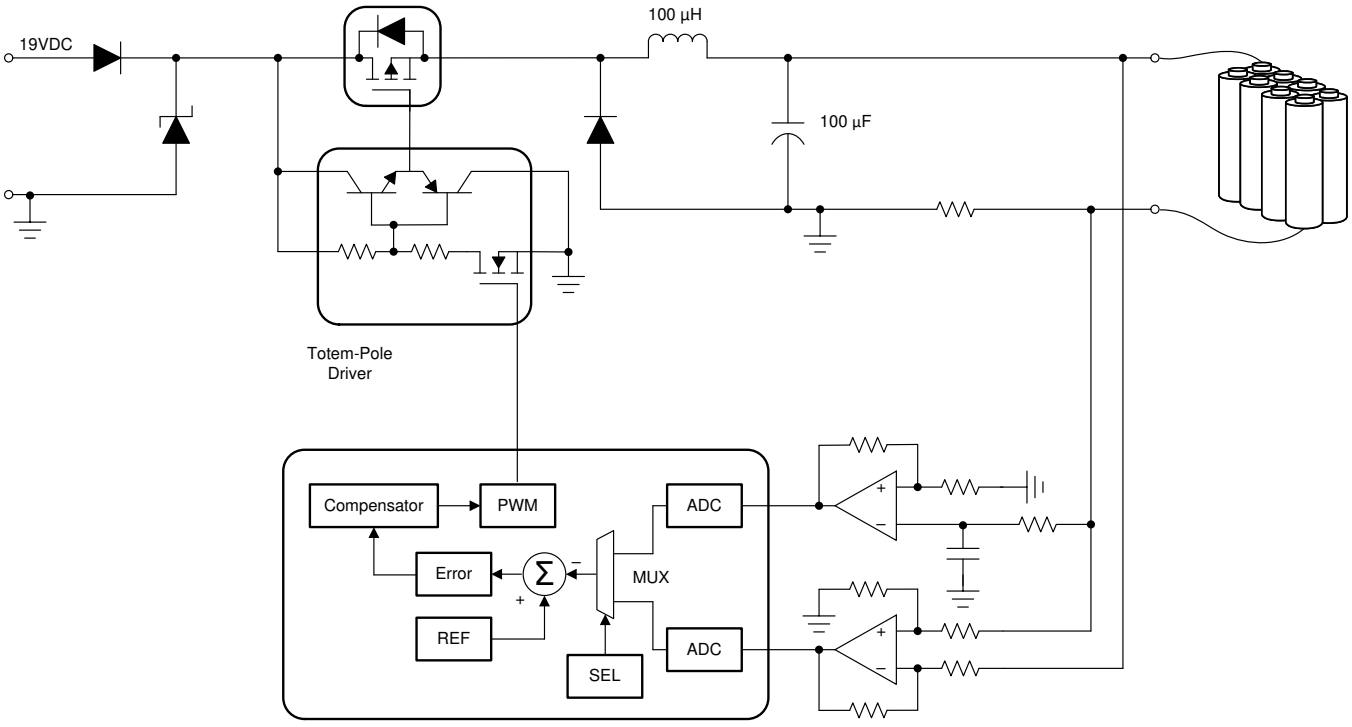

This solution is a digital-controlled, switch-mode power supply (SMPS); 'digital control' means sampling feedback information and closing the loop numerically, the error amplifier is replaced with an analog-to-digital converter (ADC) and a digital filter, the compensator uses digital-signal processing techniques to construct the control effort for the PWM.

The following items list several pros and cons of this solution:

- Limited switching frequency due to limited ADC sampling rate and Nyquist-Shannon sampling theorem, typically from 50 kHz to 100 kHz
- Large value of inductor and output capacitor needed to meet the strict output voltage regulation requirement, and large size to occupy board area
- Low efficiency due to the asynchronous buck topology and low thermal performance especially affected by the power dissipation of the free-wheeling diode
- Complex digital-signal processing techniques to achieve a stable closed loop and keep multiple MCU resources occupied, such as memory, PWM, ALU, ADC, the charging voltage accuracy depends on the accuracy of the reference voltage for ADC, and the charging voltage accuracy is around ±3%.

The other mainstream solution is using a highly-integrated battery charger IC to achieve the full charging profile with ±0.5% charging voltage accuracy. 图 2 shows the block diagram of this solution.

图 2. Integrated Onboard Charger Based on BQ24xxx

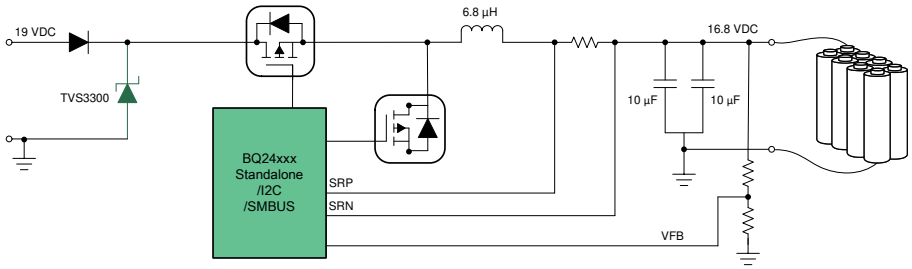

The following items list several pros and cons of this solution:

- High switching frequency from 600 kHz to 1.2 MHz, this minimizes the value of the inductor and capacitor and the layout area
- High charge current, commonly from 1.5 A to 3 A, up to 10 A, to support fast charging
- High charge voltage accuracy at ±0.5%, maximized capacity extends runtime and longer battery lifetime
- Accurate termination current, typically 10% of the charge current, maximizes capacity and extends runtime
- Built-in overcurrent, overvoltage, thermal shutdown, and FET short protections to meet strict safety criterion
- Standalone topology for easy-to-implement, and host-controlled topologies for more design flexibility

TI's BQ24xxx family is well suited for this solution, the notable products are the BQ24610, BQ24725A, and BQ24773 devices.

Meanwhile, this design provides another solution which makes trade offs between the above two solutions.

1.1 Key System Specifications

表 1. Key System Specifications

PARAMETER	SPECIFICATIONS	DETAILS
Input voltage range	17 V to 28 V	----

表 1. Key System Specifications (continued)

PARAMETER	SPECIFICATIONS	DETAILS
Number of cells in series	4S	----
Charge current	1.0A	----
Charge voltage accuracy	±1.5%	----
Charge current accuracy	±1%	----
Charge voltage ripple	±0.023%	节 3.2.2.2
Efficiency	> 90%, up to 93.5%	节 3.2.2.3
PCB size	3.0 cm × 1.8 cm	----
Operating ambient temperature	0°C to 40°C	----

2 System Overview

2.1 Block Diagram

图 3. TIDA-010075 Block Diagram

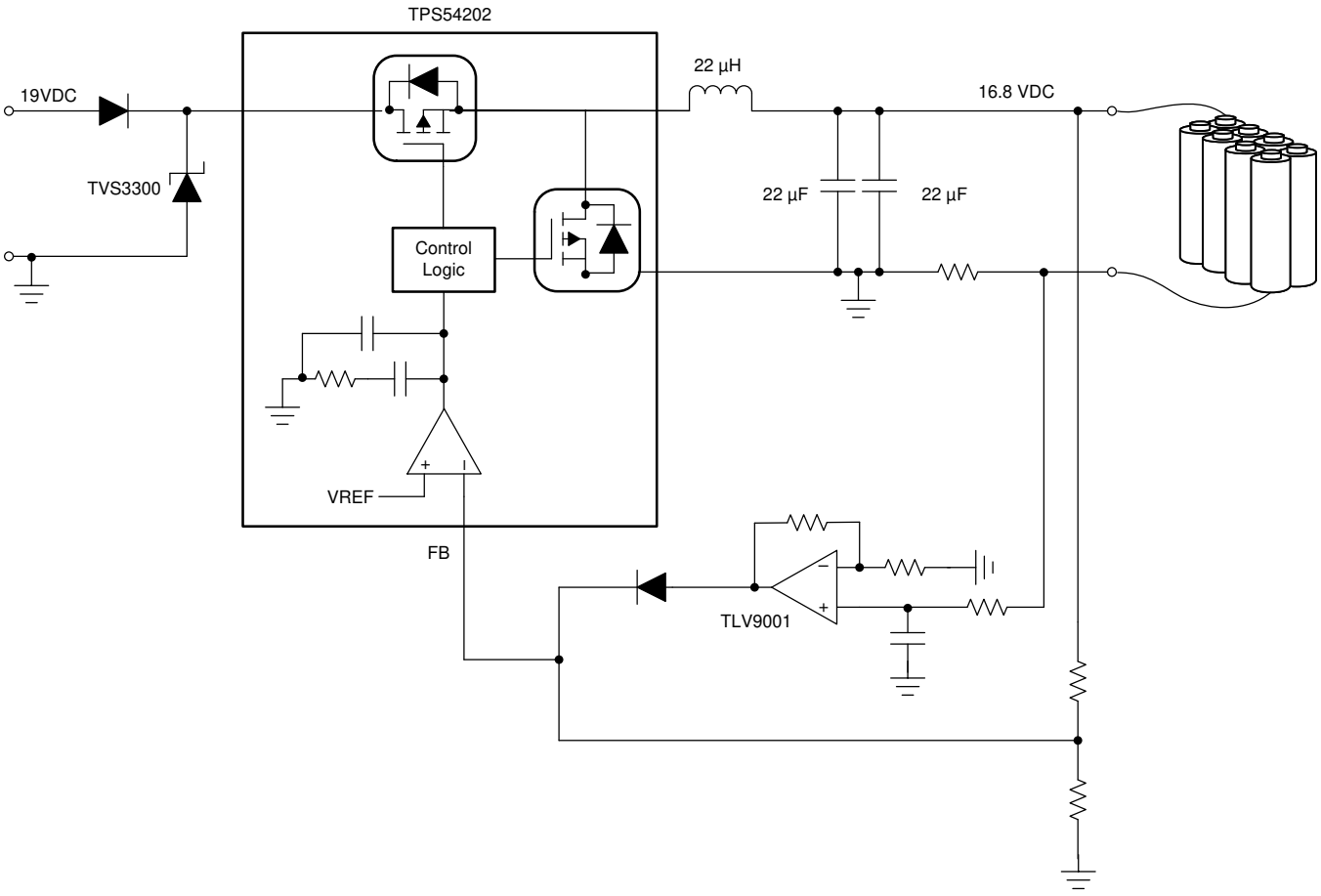

2.2 Design Considerations

This reference design attempts to optimize the system BOM cost and charge current capacity by trading-off the charge voltage accuracy, which affects the utilizable of the battery. This solution achieves a battery charger based on a synchronous buck converter - the TPS54202 device integrates two switching FETs, internal loop compensation, and employs the SOT-23 package achieving high power density and offering a small footprint on the PCB. The analog control eliminates the MCU resources and software workload, which is easier to implement and decreases the design cycle. This solution achieves a simple charging profile - constant voltage stage and constant current stage using the TLV9001 device which contributes high current-sensing accuracy.

2.3 Highlighted Products

The following subsections detail the highlighted products used in this reference design, including the key features for their selection. See their respective product data sheets for complete details on any highlighted device.

2.3.1 TPS54202

The TPS54202 is a 4.5-V to 28-V input voltage range, 2-A synchronous buck converter. The device includes two integrated switching FETs, internal loop compensation and 5-ms internal soft start to reduce component count. By integrating the MOSFETs and employing the SOT23 package, the TPS54202 device achieves the high power density and offers a small footprint on the PCB.

The device uses a fixed-frequency, peak current-mode control. The output voltage is compared through external resistors on the FB pin to an internal voltage reference by an error amplifier. An internal oscillator initiates the turn on of the high-side power switch. The error amplifier output is compared to the current of the high-side power switch. When the power-switch current reaches the error amplifier output voltage level, the high side power switch is turned off and the low-side power switch is turned on. The error amplifier output voltage increases and decreases as the output current increases and decreases. The device implements a current-limit by clamping the error amplifier voltage to a maximum level and also implements a minimum clamp for improved transient-response performance.

To reduce EMI, the TPS54202 device introduces frequency spread spectrum. The jittering span is ±6% of the switching frequency with 1/512 swing frequency. The TPS54202H device is the verison without this EMI-friendly function.

图 4. TPS54202 Functional Block Diagram

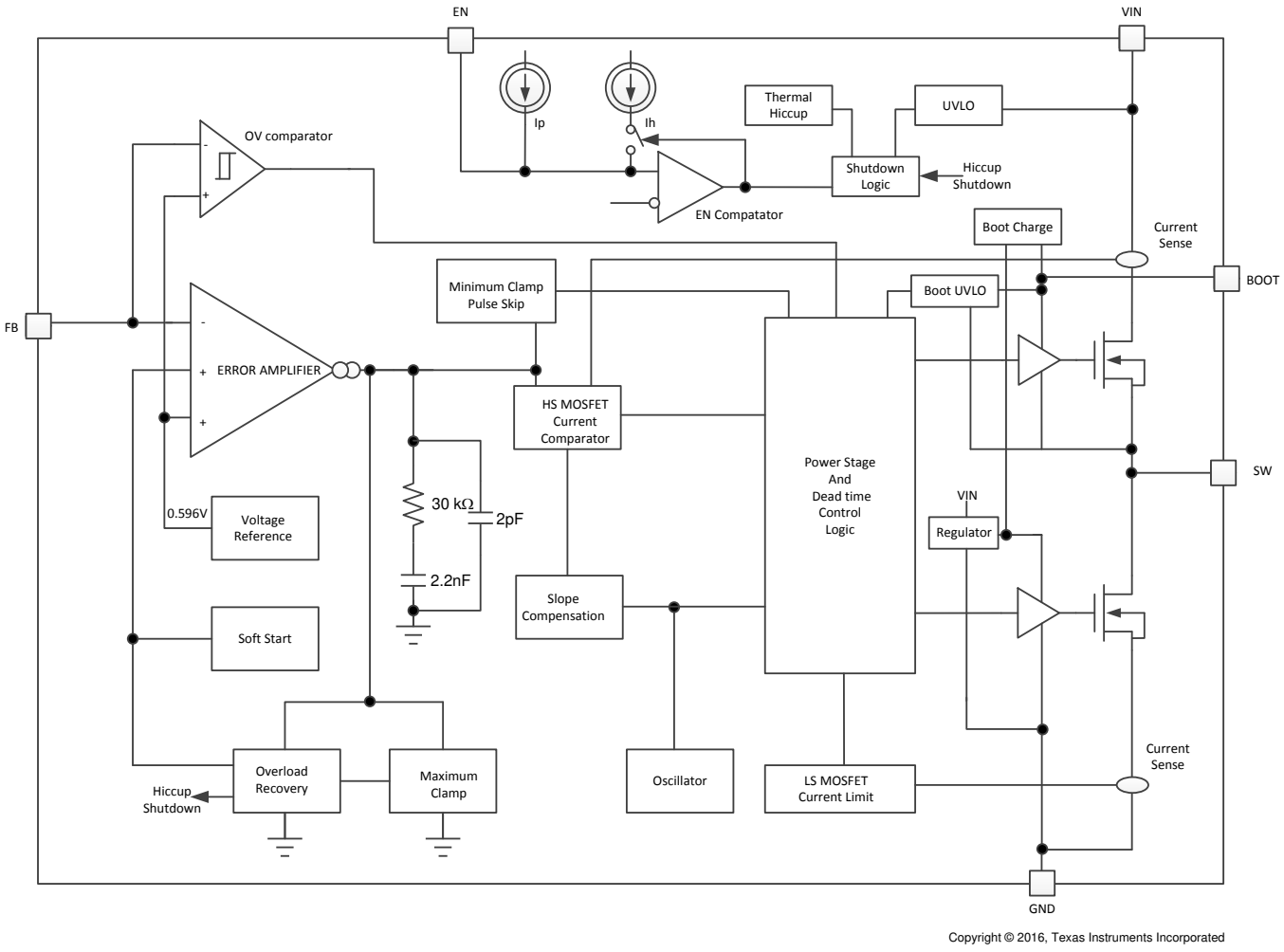

2.3.2 TLV9001

The TLV9001 device is a single channel low-voltage operational amplifier (op amps) with rail-to-rail input and output swing capabilities. This op amp provides a cost-effective solution for space-constrained applications and high capacitive-load drive is required. The capacitive-load drive of the TLV900x family is 500 pF, and the resistive open loop output impedance makes stabilization easier with much higher capacitive loads.

The robust design of the TLV900x family simplifies circuit design. The op amps feature unity-gain stability, an integrated RFI and EMI rejection filter, and no-phase reversal in overdrive conditions.

2.3.3 TVS3300

The TVS3300 device robustly shunts up to 35 A of IEC 61000-4-5 fault current to protect systems from high power transients or lightning strikes. The device offers a solution to the common industrial signal line EMC requirement to survive up to 1 kV IEC 61000-4- 5 open circuit voltage coupled through a 42-Ω impedance. The TVS3300 device uses a unique feedback mechanism to ensure precise flat clamping during a fault, assuring system exposure below 40 V. The tight voltage regulation allows designers to confidently select system components with a lower voltage tolerance, lowering system costs, and complexity without sacrificing robustness.

In addition, the TVS3300 device is available in small 1 mm × 1.1 mm WCSP and 2 mm × 2 mm SON footprints which are ideal for space-constrained applications, offering up to a 90 percent reduction in size compared to industry standard SMA and SMB packages. The extremely low device leakage and capacitance ensure a minimal effect on the protected line. To ensure robust protection over the lifetime of the product, TI tests the TVS3300 against 4000 repetitive surge strikes at high temperature with no shift in device performance.

图 5. TVS3300 Functional Block Diagram

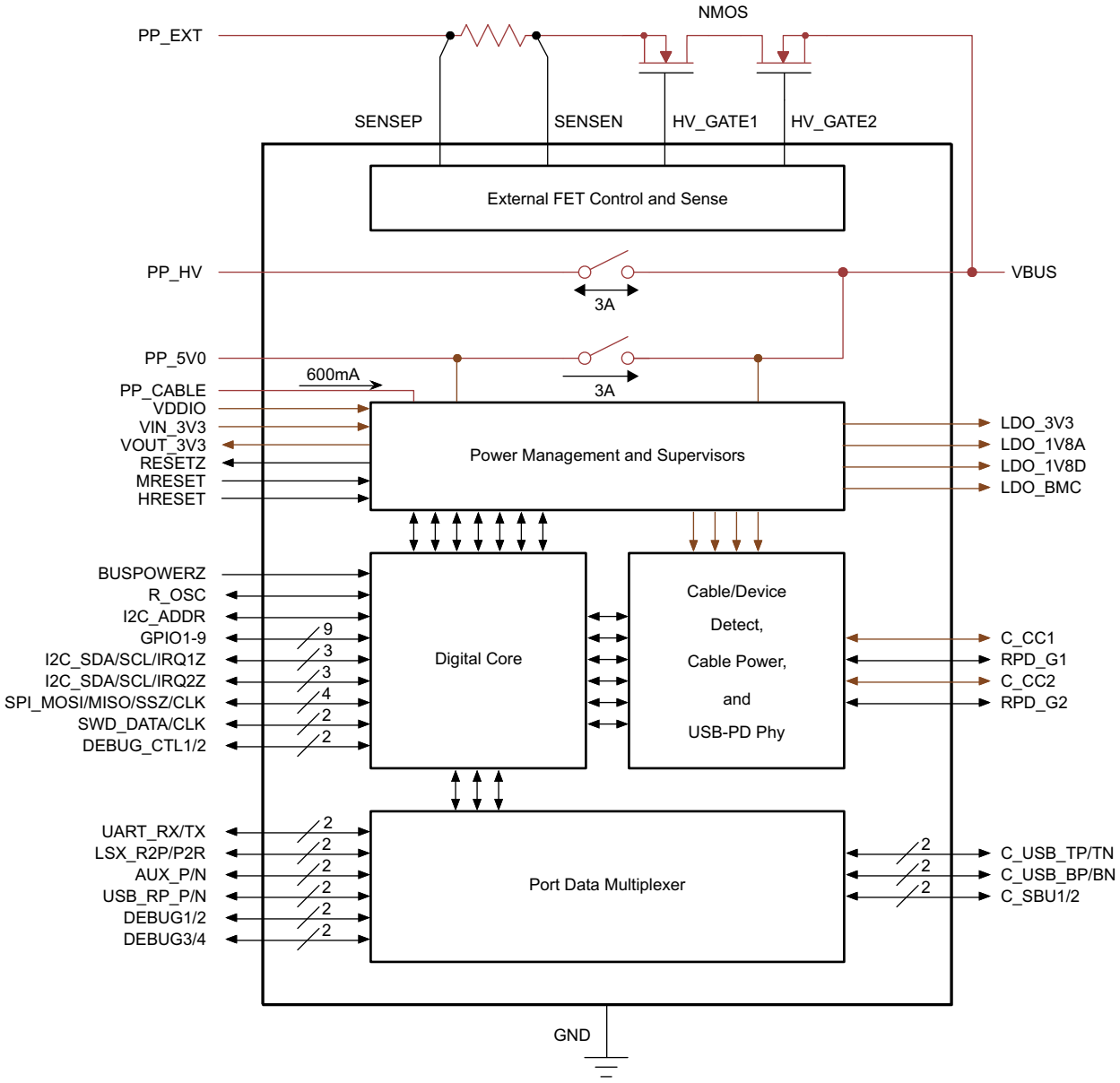

2.4 System Design Theory

To achieve the simplified charging profile, the battery charger should have both constant current (CC) control and constant voltage (CV) control. The TPS54202 device implements a constant-frequency, peak current mode control to improve line and load transients. The optimized internal compensation network minimizes the external component counts and simplified the constant voltage loop design.

2.4.1 Constant Current and Constant Voltage Control

A cost effective and simplified way to switching CV control and CC control is using one diode to achieve the OR logic function. 图 6 shows the block diagram of this implementation.

图 6. Constant Current Control Design

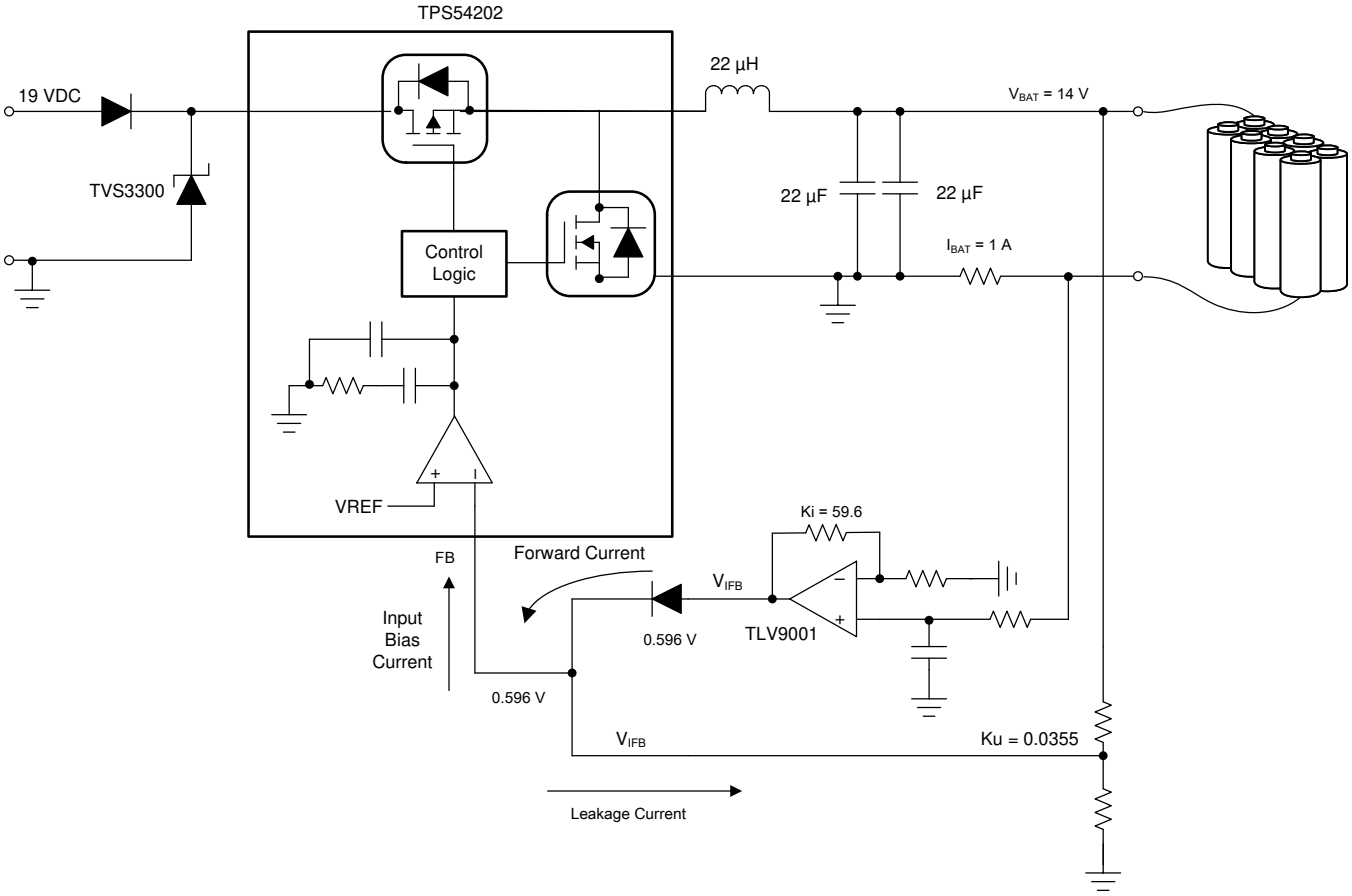

The symbols in 图 6 mean:

- V_{IFB}: the output voltage of current-sensing circuit
- V_{VFB}: the output voltage of voltage sensing circuit
- Ki : the ratio or gain between V_{IFB} and charge current, the set point is 59.6
- Ku: the ratio or gain between V_{VFB} and charge voltage, the set point is 0.0355

To better understanding the work theory of this circuit, one steady state is selected at a charge voltage of 14 V and charge current of 1 A. Thus, the related V_{IFB} is 0.596 V, and the related V_{VFB} should be 0.497 V, so the upper diode is ON, and the lower diode is OFF. According to Kirchhoff's current law (KCL), the forward current of the upper diode equals the input bias current plus leakage current of lower diode. As the input bias current is ultra low because of the high-impendence of the internal error amplifier, the dominate forward current is equal to the leakage current of the lower diode. Because the diodes should have stable forward voltage and ultra reverse current with low temperature drift, the signal Schottky barrier diode - BAT54 is selected in this design.

2.4.2 Current-Sensing Circuit

For the current-sensing circuit, a high-precision current sensor with low inductance and temperature coefficient is necessary. The CRM0805/1206-FX-R100ELF current-sense chip resistor is selected in this design, which has ±1% tolerance, ±100 ppm/°C temperature coefficient, and > 1000-MΩ insulation resistance.

This solution uses the single-supply, low-side, current-sensing solution and accurately detects load current up to 1 A, the gain required for the maximum linear output voltage depends on the required constant current value. 公式 1 shows the association between gain and the target current value.

$$V_{OUT} = \frac{V_{ref} + V_{fw}}{Gain} + I_{out} \times R_{shunt} \quad (1)$$

In this solution, the target current is 0.95 A, the internal reference voltage is 0.596 V, and the forward voltage of the diodes is 0.02 V, thus the gain of this current-sensing circuit is set at 6.482.

图 7 shows the schematic of this current-sensing circuit. For more details on how to design a single-supply, low-side, unidirectional current-sensing circuit, see the *Single-supply, low-side, unidirectional current-sensing circuit* application report.

图 7. Current-Sensing Circuit

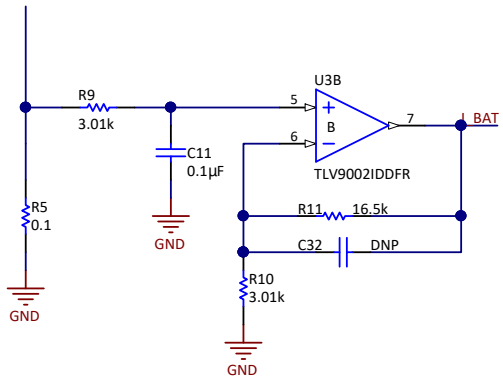

3 Hardware, Software, Testing Requirements, and Test Results

3.1 Required Hardware

图 8 shows the overview of the PCB for the TIDA-010075 design, which features:

- Two-terminal input for power supply (J1): This pin is used to connect the DC supply from the pre-stage AC/DC output voltage.
- Two-terminal output for output voltage (J2): This pin is used as the output of this charger and to connect to the battery.
- Six-terminal connector (J3): The connector is used for the external communication interface, the pin definition from left to right is: EN, M_{DAC}, I_{BAT}, GND, V_{BAT}, andVbBIAS. The EN pin is used for turning the TPS54202 device on and off, the M_{DAC} pin is optional and is used to adjust the output voltage, the I_{BAT} pin is the output of the current-sensing circuit, the V_{BAT} is the output of voltage sensing circuit, and the VbBIAS is the power supply for the op amp.

图 **8. TIDA-010075 Printed-Circuit Board**

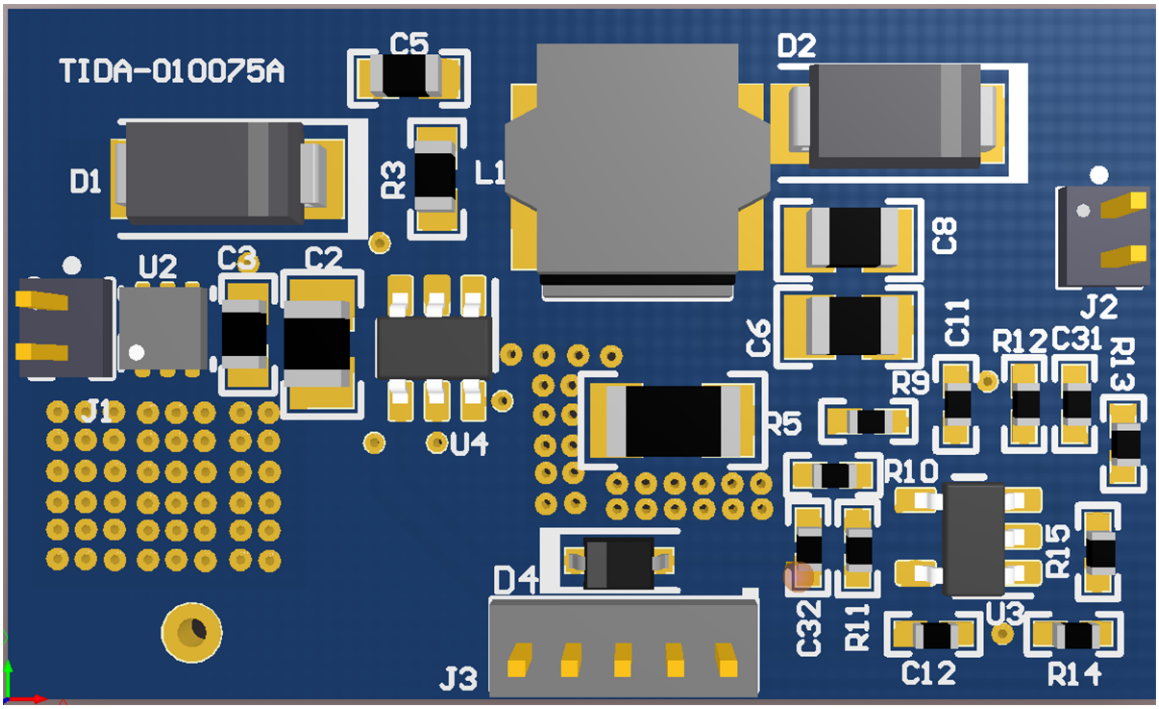

3.2 Testing and Results

3.2.1 Test Setup

表 2. Test Environment List

MATERIALS	USAGE	COMMENTS
DC Source	Power Supply	30-V, 2-A Power source
DC Source	Power Supply	6-V, 1-A Power Source
TIDA-010075 Board	Battery charger board	----
Electronic Load	Battery pack simulation	CC, CV, CR mode
Computer with PowerZ software	Collect the charging data	----
4S2P Li-Ion battery pack	Load	With protection circuit

The following steps show how to set up the test platform in the lab during the test:

1. Ensure the TIDA-010075 board has the right output voltage at no load
2. Connect the electronic load and choose the CV mode to test the constant output current
3. Connect the electronic load and choose the CC mode to test the constant output voltage

3.2.2 Test Results

3.2.2.1 CV and CC Mode Steady State

图 9 shows the steady state of constant voltage (CV) mode and 图 10 shows the steady state of constant current (CC) mode. The blue curve (CH2) is the output voltage and the purple curve (CH3) is the switching frequency. The CV mode is tested at the following conditions: output voltage at 16.5 V and the output current at 0.5 A; the CC mode is tested at the following conditions: output voltage at 15 V and output current at 0.95 A.

图 9. CV Mode Steady State

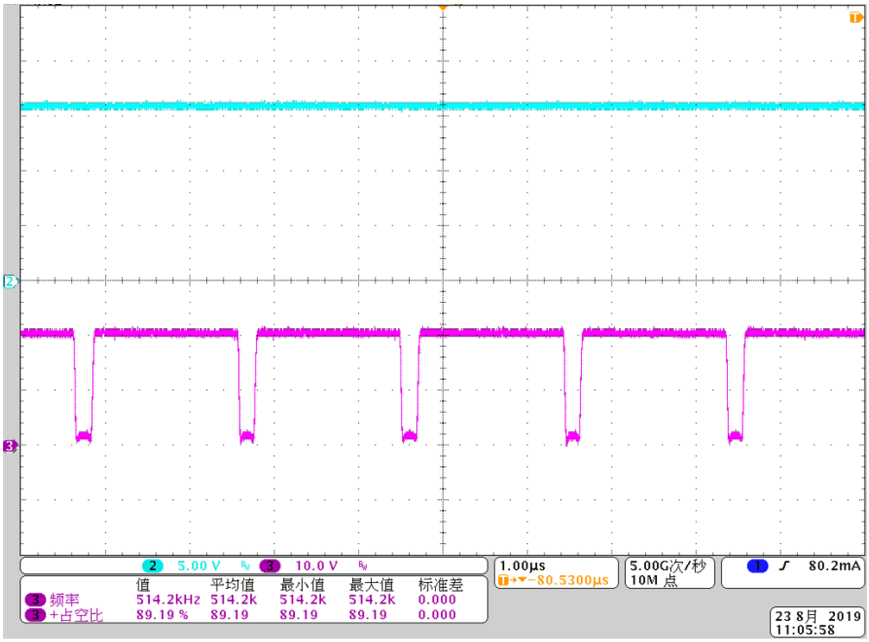

图 10. CC Mode Steady State

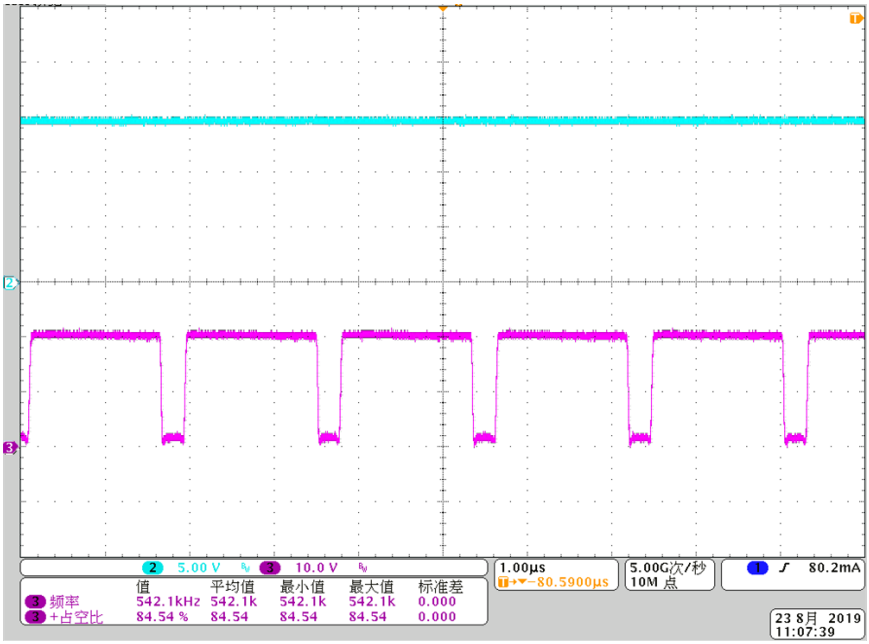

3.2.2.2 CV Voltage Ripple and CC Current Ripple

图 11 shows the voltage ripple of CV mode, and 图 12 shows the current ripple of CC mode. The output voltage ripple is less than ±3.8 mV, which also means the voltage accuracy is less than ±0.0023%. The output current ripple is tested by measuring the output voltage of the current-sensing circuit, the current ripple is less than ±12 mA. which also means the current accuracy is less than ±1.2%.

图 11. CV Mode Voltage Ripple

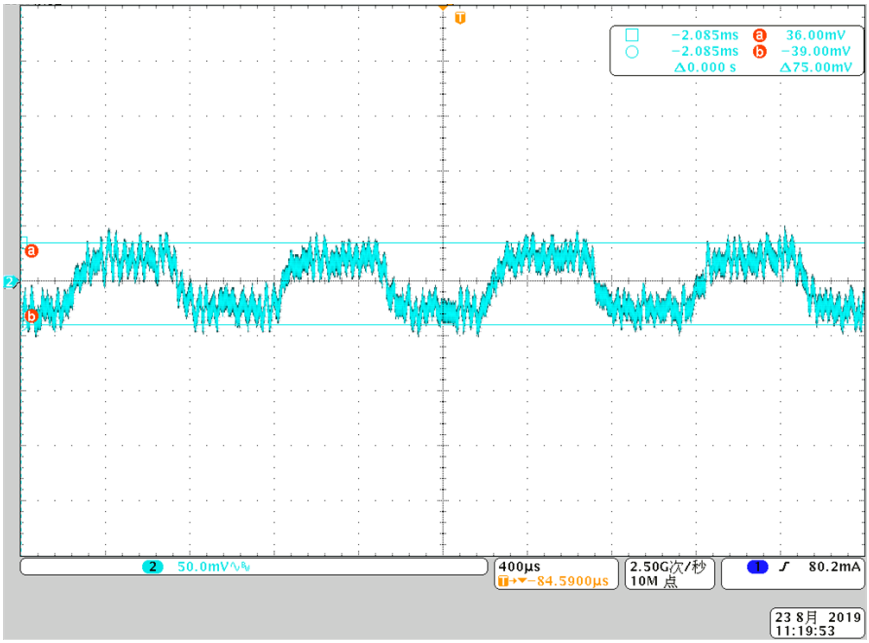

图 12. CC Mode Current Ripple

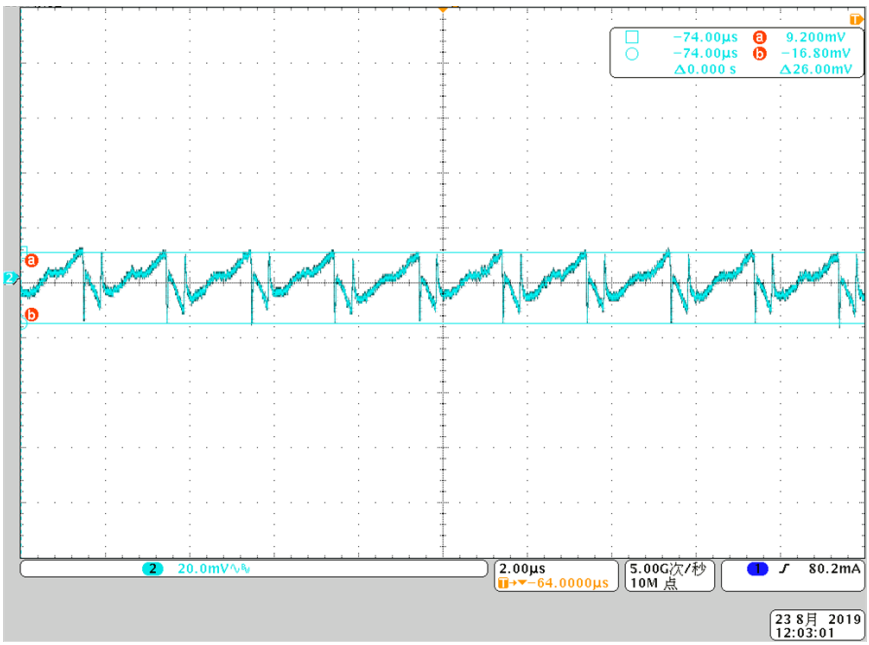

3.2.2.3 Efficiency Test

表 3 lists the test results of the efficiency of the battery charger across 0.1 A to 0.95 A.

表 3. Efficiency Test Results

INPUT VOLTAGE (V)	INPUT DC CURRENT (A)	OUTPUT VOLTAGE (V)	OUTPUT DC CURRENT (A)	EFFICIENCY (%)
18.923	0.848	15.6	0.95	92.36
18.933	0.834	16.225	0.9	92.48
18.933	0.793	16.356	0.85	92.60
18.929	0.747	16.389	0.8	92.72
18.946	0.699	16.412	0.75	92.95
18.938	0.652	16.418	0.7	93.08
18.957	0.605	16.43	0.65	93.12
18.948	0.558	16.442	0.6	93.31
18.964	0.511	16.446	0.55	93.34
18.959	0.465	16.462	0.5	97.37
18.973	0.418	16.466	0.45	93.43
18.969	0.372	16.478	0.4	93.41
18.982	0.325	16.483	0.35	93.51
18.982	0.279	16.496	0.3	93.44
18.992	0.233	16.505	0.25	93.25
18.992	0.188	16.515	0.2	92.51
19.001	0.142	16.522	0.15	91.85
19.003	0.097	16.534	0.1	89.70

图 13 shows the efficiency curve of these test conditions.

图 13. Efficiency Versus Output Current

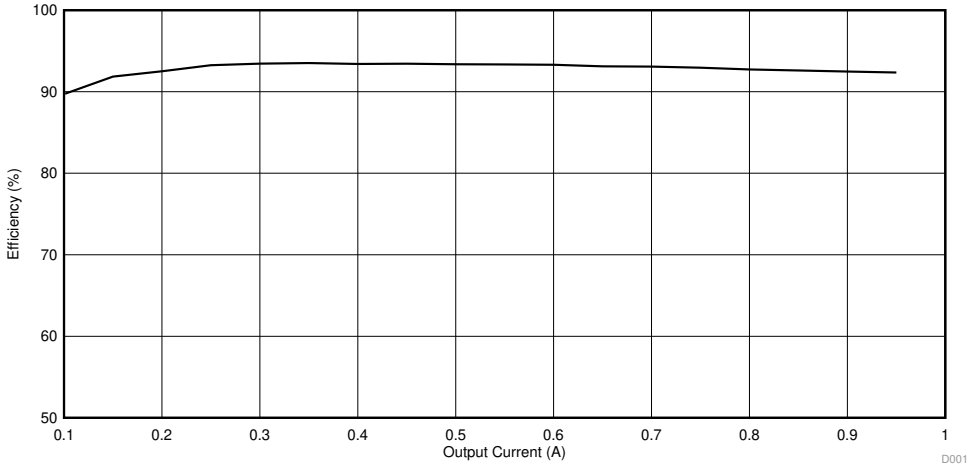

3.2.2.4 Thermal Test

图 14 shows the thermal image of the board after 10 minutes of continuous running. The maximum temperature observed on the TPS54202 device is 75.7°C, and the maximum temperature on the input reverse current protection diode is 80.6°C.

图 **14. Thermal Test**

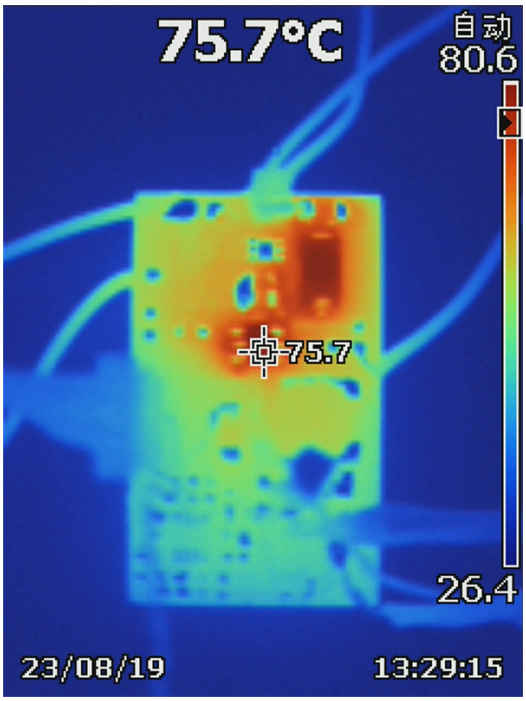

3.2.2.5 Voltage and Current Close Loop Stability

图 15 shows the voltage close loop stability performance of TIDA-010075 reference design, the gain crossover frequency is 19.68 kHz, and the phase margin is 65.045°, which means this control circuit is stable and can provide enough bandwidth.

图 **15. Voltage Close Loop Stability**

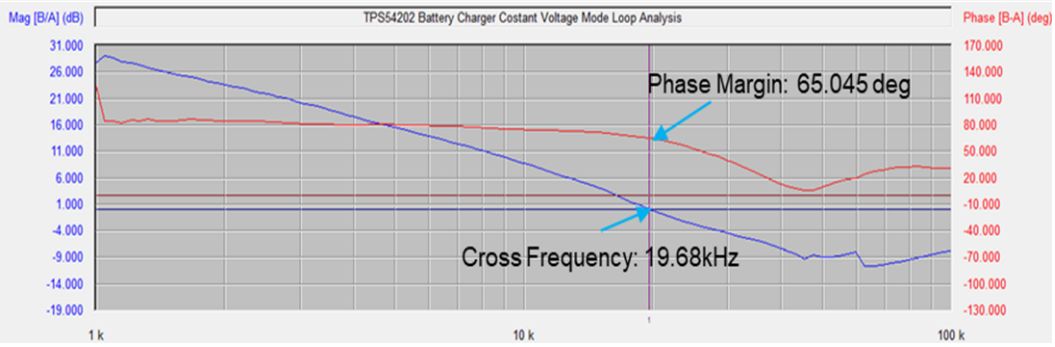

图 16 shows the current close loop stability performance of TIDA-010075 reference design, the gain crossover frequency is 15.28 kHz, and the phase margin is 51.886°, which means this control circuit is stable and can provide enough bandwidth.

图 16. Current Close Loop Stability

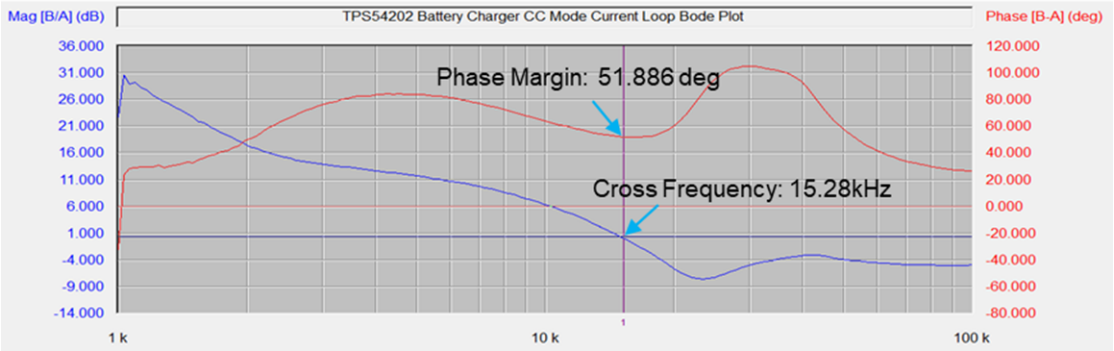

3.2.2.6 *Charging Profile*

图 17 shows the charging profile of this solution, the load is using a 4S2P battery pack with protection circuit.

图 17. Charging Profile

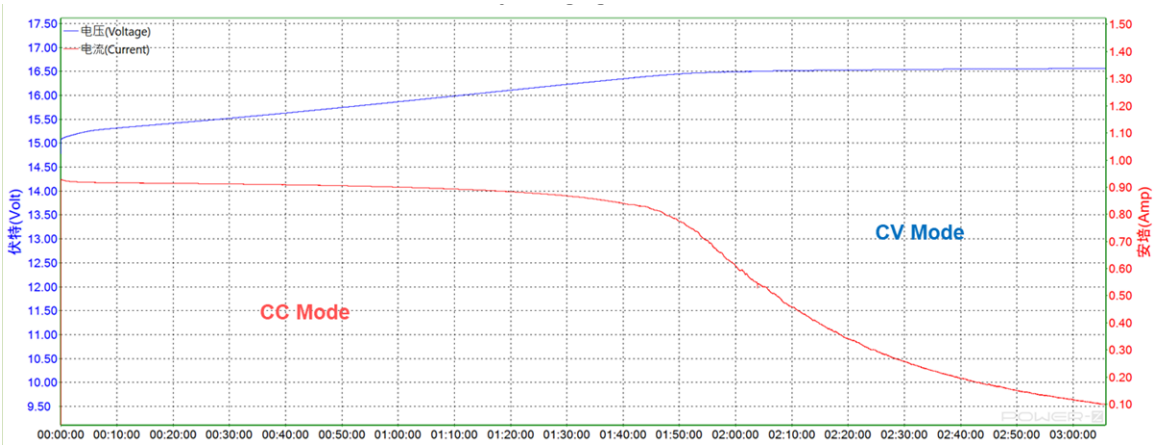

The charging profile consists of CV mode and CC mode, the transformation between CC to CV is smooth and stable.

4 Design Files

4.1 Schematics

To download the schematics, see the design files at TIDA-010075.

4.2 Bill of Materials

To download the bill of materials (BOM), see the design files at TIDA-010075.

4.3 PCB Layout Recommendations

4.3.1 Layout Prints

To download the layer plots, see the design files at TIDA-010075.

4.4 Altium Project

To download the Altium Designer® project files, see the design files at TIDA-010075.

4.5 Gerber Files

To download the Gerber files, see the design files at TIDA-010075.

4.6 Assembly Drawings

To download the assembly drawings, see the design files at TIDA-010075.

5 Software Files

To download the software files, see the design files at TIDA-010075.

6 Related Documentation

1. Texas Instruments, *TPS54202 4.5-V to 28-V Input, 2-A Output, EMI Friendly Synchronous Step Down Converter Data Sheet*
2. Texas Instruments, *TLV900x Low-Power, RRIO, 1-MHz Operational Amplifier for Cost-Sensitive Systems Data Sheet*
3. Texas Instruments, *TVS3300 33-V Flat-Clamp Surge Protection Device Data Sheet*
4. Texas Instruments, *Single-supply, low-side, unidirectional current-sensing circuit application report*
5. Texas Instruments, *Difference amplifier (subtractor) circuit application report*

6.1 商标

6.2 Third-Party Products Disclaimer

7 About the Author

ZHILONG (BRYAN) LIU is a system engineer at Texas Instruments, responsible for developing subsystem design solutions for the industrial appliances systems. He has system-level product experience in analog and mixed-signal designs. Bryan earned his Bachelor of Technology in electrical and information engineering from Xidian University, and his Master of Technology in circuit and system from Xidian University.

重要声明和免责声明

TI“按原样”提供技术和可靠性数据（包括数据表）、设计资源（包括参考设计）、应用或其他设计建议、网络工具、安全信息和其他资源，不保证没有瑕疵且不做出任何明示或暗示的担保，包括但不限于对适销性、某特定用途方面的适用性或不侵犯任何第三方知识产权的暗示担保。

这些资源可供使用 TI 产品进行设计的熟练开发人员使用。您将自行承担以下全部责任：(1) 针对您的应用选择合适的 TI 产品，(2) 设计、验证并测试您的应用，(3) 确保您的应用满足相应标准以及任何其他功能安全、信息安全、监管或其他要求。

这些资源如有变更，恕不另行通知。TI 授权您仅可将这些资源用于研发本资源所述的 TI 产品的应用。严禁对这些资源进行其他复制或展示。您无权使用任何其他 TI 知识产权或任何第三方知识产权。您应全额赔偿因在这些资源的使用中对 TI 及其代表造成的任何索赔、损害、成本、损失和债务，TI 对此概不负责。

TI 提供的产品受 TI 的销售条款或 ti.com 上其他适用条款/TI 产品随附的其他适用条款的约束。TI 提供这些资源并不会扩展或以其他方式更改 TI 针对 TI 产品发布的适用的担保或担保免责声明。

TI 反对并拒绝您可能提出的任何其他或不同的条款。

邮寄地址：Texas Instruments, Post Office Box 655303, Dallas, Texas 75265